A maximum likelihood method for partial volume segmentation of magnitude breast MR data

M. Freed[1,2], C. Graff[1], M. I. Altbach[3], J. A. de Zwart[4], J. H. Duyn[4], and A. Badano[1]
[1]CDRH/OSEL/DIAM, FDA, Silver Spring, MD, United States, [2]Department of Bioengineering, University of Maryland, College Park, Maryland, United States, [3]Department of Radiology, University of Arizona, Tucson, Arizona, United States, [4]NINDS/LFMI/Advanced MRI Section, National Institutes of Health, Bethesda, MD, United States

Introduction: Women with a greater amount of dense breast tissue have a higher risk of developing breast cancer than women with fattier breast tissue [1-3]. Traditionally, breast density is clinically measured using x-ray mammography, which is a two-dimensional imaging technology, however three-dimensional modalities, such as MR, may provide more accurate estimates of breast density [4,5]. Breast density can be estimated by using segmentation algorithms to separate adipose and glandular tissues in an image. There exist a large variety of methods for image segmentation in MR including algorithms based on intensity thresholding, clustering, and Dixon techniques [6-9]. In breast MR, these methods are typically applied to the signal intensities in pre-contrast, T_1-weighted images. In this study, we apply maximum likelihood (ML) estimation techniques to magnitude images as a method for image segmentation. This method is based on the signal equation of the acquired data and, therefore, takes into account some of the physics of the data acquisition process. We validate the method on simulated data and then apply it to physical phantom data.

Methods: A simulated breast phantom was created based on in vivo computed tomography (CT) data and used to generate noisy MR inversion recovery (IR) and saturation recovery (SR) magnitude images. A segmentation algorithm based on ML estimation was applied to estimate the partial volume segmentation that was then compared with the truth. This algorithm was also applied to physical IR phantom data. ***Simulated phantom data:*** An intensity threshold was applied to an anonymous, archived, human, dedicated breast CT data set (binned to planar res. = 1.348 mm, slice thick. = 0.207 mm) to approximately separate the adipose and glandular tissue types. Twenty-one contiguous slices were then combined to create a single simulated MR axial slice, where the phantom's true glandular fraction per voxel (GFPV) was determined by the number of CT slices that contained adipose and glandular tissue at that location. Simulated IR and SR data were created by applying a double-exponential signal equation ($T_{1adipose}$=240 ms, $T_{1glandular}$=1290 ms, equilib. signal for all glandular or all adipose=1.0) for a set of inversion or repetition times (TI or TR=[35, 50, 75, 100, 150, 250, 400, 600, 900, 1500, 3000, 9000] ms) and adding noise (var.=2.5e-5) to each simulated image. Data for the IR experiment takes several hours to acquire and might be used to characterize phantoms, however the SR data can be acquired with a fast spin-echo sequence in approximately 9 minutes and is more clinically relevant. ***Segmentation algorithm:*** Magnitude MR images have Rician-distributed noise [10]. The likelihood equation for Rician-distributed data has been previously derived [11] and can be used to estimate parameters of the MR image signal equation. Since adipose and glandular tissues have significantly different T_1 values, we can use a T_1 sensitive imaging sequence to discriminate between them. We have applied the segmentation algorithm to both IR and SR data using double-exponential signal equations to account for the two tissue types in the breast. The concentrations of the two tissue types (and, therefore, the fraction of glandular material in a voxel) as well as the T_1 of the glandular tissue were estimated by maximizing the likelihood of the measured data. We assume that the T_1 value of the adipose tissue is a known quantity; this can be determined separately using a monoexponential signal equation on a region with no glandular tissue. The maximization of the likelihood was implemented using a limited-memory Broyden-Fletcher-Goldfarb-Shanno method with bounds [12] in the R programming language. ***Physical phantom and data:*** The physical phantom was constructed using lard to simulate adipose tissue and coagulated fresh egg whites to simulate fibroglandular tissue [13]. A preservative was added to the egg whites before they were poured into melted lard and allowed to coagulate. The mixture was then cooled at room temperature in a sealed plastic jar. This procedure resulted in a random structure with a different glandular/adipose fraction in each voxel. IR scans (TI=[35, 50, 75, 100, 150, 250, 400, 600, 900, 1500, 3000, 9000] ms, TE=15 ms, TR=10 s, resolution= 1x1x3 mm^3) were performed on a Siemens Magnetom 1.5 T clinical scanner using a knee coil. For lard, the T_1 value was estimated on a tube of solid lard assuming monoexponential signal behavior.

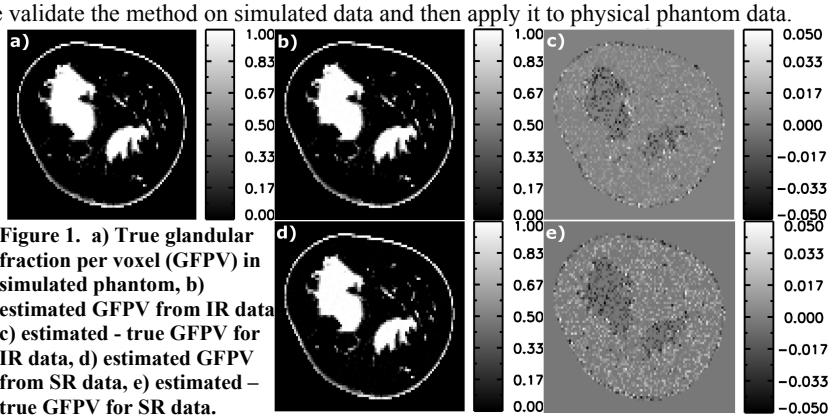

Figure 1. a) True glandular fraction per voxel (GFPV) in simulated phantom, b) estimated GFPV from IR data c) estimated - true GFPV for IR data, d) estimated GFPV from SR data, e) estimated – true GFPV for SR data.

Results: Figure 1 shows the results of the analysis on the simulated data for the IR and SR experiments, showing the true GFPV, the estimated GFPV generated by applying the ML segmentation algorithm to the IR and SR data, and the absolute difference between the true and estimated GFPV. The algorithm accurately segments the two tissue types in the presence of noise. Figure 2 shows the results of the segmentation algorithm applied to the physical phantom data. Both the MR data and estimated GFPV are shown.

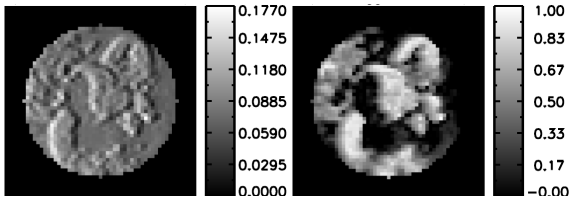

Figure 2. (left) Acquired IR data on physical phantom (TI = 9000 ms) (right) Estimated GFPV.

Conclusions: We have demonstrated that the ML segmentation algorithm is able to successfully separate tissue types in both simulated and phantom MR images. In the future we plan to apply this to human data and perform a quantitative comparison with other partial volume segmentation algorithms currently being used. This technique incorporates an imaging physics model and is insensitive to field inhomogeneities; advantages which may improve tissue separation compared to other methods.

Acknowledgments: John Boone for human CT data, Brandon Gallas and Kyle Myers for discussions, funding from the FDA/OWH, supported by an appointment to CDRH/ORISE. **References:** [1] Wolfe, Cancer, 37, 2486, 1976 [2] Threatt et al., Cancer, 45, 2550, 1980 [3] Vacek and Geller, Cancer Epidemiol Biomarkers Prev., 13, 715, 2004 [4] Yaffe, Breast Cancer Res., 10, 209, 2008 [5] Lee et al., AJR, 168, 501, 1997 [6] Bezdek, Hall, and Clarke, Med. Phys., 20, 4, 1033, 1993 [7] Clarke et al., MRI, 13, 343, 1995 [8] Pham, Xu, and Prince, Annu. Rev. Biomed. Eng., 2, 315, 2000 [9] Glover and Schneider, MRM, 18, 371, 2005 [10] Gudbjartsson and Patz, MRM., 34, 910, 1995 [11] Karlsen, Verhagen, and Bovee, MRM, 41, 614, 1999 [12] Byrd et al., SIAM J. Sci. Comput., 16, 1190, 1995 [13] Freed et al., RSNA, SSE21-01, 2009